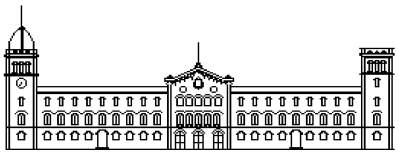

Treball final de grau

GRAU DE MATEMÀTIQUES

Facultat de Matemàtiques
Universitat de Barcelona

FRACTALS: OBJECTS TO BETTER EXPLAIN OUR WORLD

Jordi A. Cardona Taltavull

Director: Nuria Fagella Rabionet
Realitzat a: Departament de Matemàtiques i Informàtica. UB

Barcelona, 29 de Juliol de 2017

Abstract

In this paper we will look at some properties fractals and show the usefulness of one of them, the fractal dimension, for the study of natural and artificial phenomena. We will center our attention on fractals generated by Iterated Function Sets (IFS), which we will define as a system of contractive mappings on non-empty compact sets in a complete metric space.

First, we will present some simple, well known, fractals, and show how to generate them with a geometrical construction. To compute these objects, we will use two distinct algorithms based on the iteration of IFS, a deterministic and a random one.

We will then see an application of the fixed point theorem for IFS, named the Collage Theorem. We will show that an IFS's attractor is unique and independent of the initial set. Moreover, we will show that both the deterministic and the random algorithms converge to the same limit: the attractor of the system.

Having studied fractals generated by IFS, we will go on to look at fractal dimensions. For this purpose we will review the classic concept of dimensions, and broaden it to include non-integer dimension. We will see different types of fractal dimensions, some of which are suited to a specific type of fractals, such as the self-similarity dimension applicable to self-similar shapes, and a more general dimension, applicable to any fractal, namely, the Hausdorff-Besicovitch Dimension. We will also see the Box-counting algorithm, which approximates the Hausdorff-Besicovitch Dimension and is often used in its stead because of the complexity of calculating the dimension.

We will conclude our exploration of fractal dimensions with the presentation of a small personal contribution to this area – our own version of a program which implements the box-counting algorithm on images.

In the last chapter we will see some examples of the practical uses of the fractal dimension in fields of study as diverse as medicine, market research, image classification and so on. Through these examples we can appreciate the impact of fractals on our way of modeling or explaining our world.

Contents

"...What do you consider the largest map that would be really useful?"
"About six inches to the mile."
""Only six inches!" exclaimed Mein Herr.
"We very soon got to six yards to the mile. Then we tried a hundred yards to the mile. And then came the grandest idea of all! We actually made a map of the country, on the scale of a mile to the mile!"
"Have you used it much?" I enquired.
"It has never been spread out, yet," said Mein Herr: "the farmers objected: they said it would cover the whole country, and shut out the sunlight! So we now use the country itself, as its own map, and I assure you it does nearly as well."

From *Sylvie and Bruno Concluded* by Lewis Carroll, first published in 1893.

1 Introduction

A pattern in the noise

Around 1958 Benoit Mandelbrot (1924-2010) initiated an investigation of noise analysis and electric disturbances in the IBM lab. He noticed a behavior pattern in what should have been random noise, which, moreover, repeated on various scales. Having previously studied the work of Gaston M. Julia (1893-1978) and Georg Cantor (1845-1918), he tried to apply their discoveries, especially the Cantor Set, in order to simulate the behavior of the noise fluctuation, and found they fit.

Irregular measurements do not necessarily effect an overall structure on a larger scale, but ignoring them results in a simplified model. But what if we wish to maintain the complexity of a natural object, how do we measure it? Mandelbrot arrived at a simple question which exemplifies his discovery, which is:

How long is the coast of Britain?[10]

Figure 1.1: Britain

This question may seem absurd, but is nonetheless a classic example of this type of application: The Coastline Paradox.

The length of a coastline is not a constant, but a function of scale, that is, the distance from which you observe. It is not the same to observe the coast

from a satellite, from an airplane, or from ground level. The measurement, in each case, would give a different result, since it is easy to demonstrate that a figure with straight edges is shorter than the same figure with rough edges. The more finely you measure, the longer the coastline seems to get (Figure 1.2).

Figure 1.2: Britain's coastline measures

We simplify the world in order to describe it, break it down into components of lesser complexity. The common figures of classic or Euclidean geometry are sufficient in most cases in order to approximate reality and achieve working models of it. Nonetheless, these figures prove inadequate if we wish to generate accurate models of complex forms like the leaf of a tree or the profile of a mountain. Their limitation is due to their tendency to lose their structure when they are amplified. The arch of a circumference turns gradually into a straight line, the surface of a sphere becomes flatter, etc. Although natural forms seem to lose structure when scaled, close observation shows that they do not. For example, the rough surface of a rock maintains practically the same complexity through several levels of amplification. If we analyze part of the rock, and within it a smaller part, and a smaller one still, it will not seem to become smoother.

Now we can ask ourselves, is there another way to describe these entities, which maintains their properties and characteristics at any scale? Could we not describe them through objects which take this property of detail to the extreme, forms which, though much more complicated then traditional geometric figures, may be constructed by a simple procedure?

The answer to these questions is the subject of this paper: fractals.

From monsters to (top) models

In 1975 Mandelbrot coined the term 'fractal', from the Latin *fract* o *fractus*, meaning "broken" or "uneven". In his book, *The fractal geometry of nature*[11], Mandelbrot famously states ¨ clouds are not spheres, mountains are not cones, coastlines are not circles, and bark is not smooth, nor does lightning travel in a straight line¨, popularizing the idea of fractals, and gaining acclaim as the father of the field. Although he may have been the first to see the

possible applications of these complex shapes in modeling natural objects, the mathematical studies which enabled his discovery precede him by more the a century.

As early as 1872, Karl Weierstrass (1815-1897) discovered a function (Figure 1.3) which is continuous everywhere, but nowhere differentiable. Historically, the Weierstrass function is important, being the first published example challenging the notion that every continuous function is differentiable except on a set of isolated points. This function is relevant to the fractal geometry because it is the first to exhibit one of the most well known properties of fractals, which we will later introduce: self-similarity.

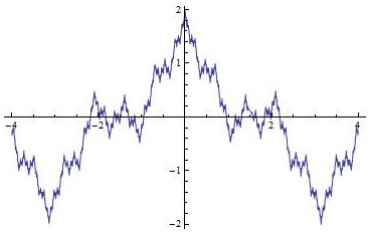

Figure 1.3: Weierstrass Function

In 1883, Georg Cantor, famous as one of the creators of the Set Theory, introduced objects we now see as fractals, in the course of his investigation of transfinite numbers. His work was so ahead of its time that even renowned mathematicians, such as Henry Poincaré and Leopold Kronicker, harshly criticized it. Cantor's objects, and others, such as Koch's Curve and Sierpinski's Triangle, seemed so strange that they were referred to as 'monsters'. Nonetheless, their importance is now widely recognized. Later, in Chapter 2, we will take a closer look at these objects and others, see some of their properties and how they are constructed.

In 1917 Felix Hausdorff (1868-1942) generalized the idea of length, area and volume - the Lebesgue outer measures, - with the measure that bears his name. This measure is the basis for a new definition of dimension, which includes fractional values for objects which defy conventional integer dimensions. Much of the theoretical work on this dimension was carried out by Abram Besicovitch, which is why the dimension is named the Hausdorff-Besicovitch dimension. The applications of this concept are currently the topic of lively investigation in a wide variety of fields, ranging from Chaos Theory through eminently practical pattern recognition applications in medicine and biometrics, and image compression in cinema.

And speaking of cinema (we did promise top models), we cannot conclude our review of important mathematical contributions to the study of fractals without mentioning Michael Barnsley (1946), discoverer of the Collage Theorem [1]. Following Mandelbrot's identification of fractals in many natural phenomena, Barnsley aspired to do the contrary – for any given image, find the appropriate fractal functions which would generate it. In the course of this

endeavor, he has made important advances in the compression and generation of fractal images. His work enabled the creation of fractals of artistic value we now know as fractal art, fractal generated models for cinema, and much more.

The closer you get

When we speak of fractals, what immediately comes to mind is their property of self-similarity. Mandelbrot originally defined a fractal as a semi-geometrical object who's basic, fragmented or irregular, structure, repeats itself on different scales. He refers to it as semi-geometrical since it is more complex then a regular geometric object, and the repetition of structure refers to its property of self-similarity. Mandelbrot considered an object is self-similar if its parts had the same form or structure as the whole, even though these may be slightly deformed. This property can be seen clearly if we observe one of the most famous fractals: Sierpinski triangle or Sierpinski Gasket (Figure 1.4).

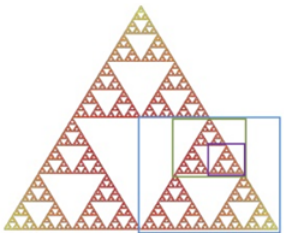

Figure 1.4: Sierpinski Gasket

We can see the triangle is formed by three smaller triangles, each one of those, for example the bottom right one, in the square, is identical up to scale to the original triangle. Going smaller and smaller in scale, we will discover triangles which are, in turn, formed by smaller triangles and are identical to the original triangle. Theoretically, this can go on infinitely as we reduce the scale.

But as we said, self-similarity does not necessarily mean that parts are copies of the whole. in the following fractal set, the Mandelbrot Set (Figure 1.5), we can see that the pieces do not coincide perfectly on all scales, but the structural similarity is present in all of them so it is considered self-similar.

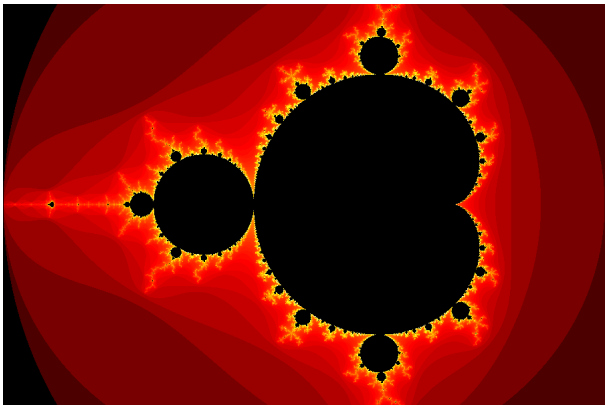

Figure 1.5: Mandelbrot Set [11]

Althogh self-similarity is typical of fractals, using it as a definition seems insufficient.

Objects to better explain our world

Falconer[4] considers it best to regard a fractal as a set that has properties such self-similarity, and others, listed below, rather than look for a precise definition which will almost certainly exclude some interesting cases. He proposes that when we refer to a set as a fractal, we have the following in mind. (i) it has a fine structure, i.e. detail on arbitrarily small scales. (ii) it is too irregular to be described in traditional geometrical language, both locally and globally. (iii) it has some form of self-similarity, perhaps approximate or statistical. (iv) its 'fractal dimension' is greater than its topological dimension. (v) In most cases of interest it is defined in a very simple way, perhaps recursively.

In this paper we will look at some of these properties, and show the usefulness of one of them, the fractal dimension, for the study of natural and artificial phenomena. We will center our attention on fractals generated by Iterated Function Sets (IFS), which we will define as a system of contractive mappings on non-empty compact sets in a complete metric space.

First, we will present some simple, well known, fractals, and show how to generate them with a geometrical construction. To compute these objects, we will use two distinct algorithms based on the iteration of IFS, a deterministic and a random one.

The deterministic algorithm consists in applying all functions of an IFS at each iteration of the process. The random algorithm, on the other hand, applies a random sequence of equivalent functions on a given point, generating a sequence of points. The selection of these functions may be determined by a set of probabilities, that is to say, each function will have a certain probability of being selected.

We will then see an application of the fixed point theorem for IFS, named the Collage Theorem. We will show that an IFS's attractor is unique and inde-

pendent of the initial set. Moreover, we will show that both the deterministic and the random algorithms converge to the same limit: the attractor of the system. That is to say, the sequence generated by the random algorithm will pass through all the points of the attractor of the deterministic algorithm, or very close to them (in terms of the Hausdorff distance).

Having studied fractals generated by IFS, we will go on to look at fractal dimensions. For this purpose we will review the classic concept of dimensions, and broaden it to include non-integer dimension. We will see different types of fractal dimensions, some of which are suited to a specific type of fractals, such as the self-similarity dimension applicable to self-similar shapes, and a more general dimension, applicable to any fractal, namely, the Hausdorff-Besicovitch Dimension. We will also see the Box-counting algorithm, which approximates the Hausdorff- Besicovitch Dimension [2] and is often used in its stead because of the complexity of calculating the dimension.

We will conclude our exploration of fractal dimensions with the presentation of a small personal contribution to this area – our own version of a program which implements the box-counting algorithm on images.

In the last chapter we will see some examples of the practical uses of the fractal dimension in fields of study as diverse as medicine, market research, image classification and so on. Through these examples we can appreciate the impact of fractals on our way of modeling or explaining our world.

2 Some simple fractals

In this section we will see the construction of some fractals using an initiator set and generator set, and an affinity iteration.

2.1 The Sierpinski Gasket

In order to construct this fractal, we start with a black triangle on a white background (Figure 2.1), then iterate the following process: for each black triangle, we shall join the middle points of each side and eliminate the resulting triangle.

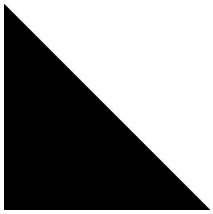

Figure 2.1: Sierpinski Gasket. Initiator set

Iterating this process, results, at the limit, in the Sierpinski triangle (Figure 2.2).

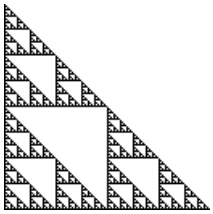

Figure 2.2: Iteration's limit: Sierpinski Triangle

The triangle is self-similar since, as we can see, it is made out of smaller and smaller copies of itself.

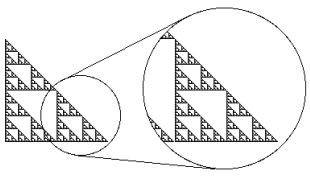

Figure 2.3: Self-similarity of the triangle.

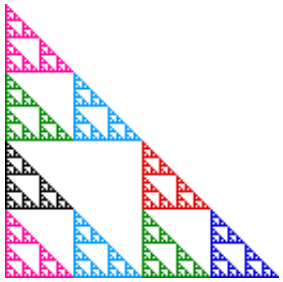

Figure 2.4: Each color is one of the nine copies of the original shape

That is to say, we can describe the triangle as made out of three copies, each one half the height and width of the original triangle (Figure 2.3). In turn, each one of these copies will be made up of three, even smaller copies. Therefore we may say the triangle has in itself nine copies of a quarter of its height and width (Figure 2.4). Or twenty seven with an eight of its height and width, and so on.

2.2 The Koch Curve

Another basic fractal is the Koch Curve. Taking as initiator a segment of a line with the length of 1, and as generator the form resulting from eliminating the central third of the line and adding two segments of the same length which would form an equilateral triangle with the segment previously eliminated, as we see in the Figure 2.5

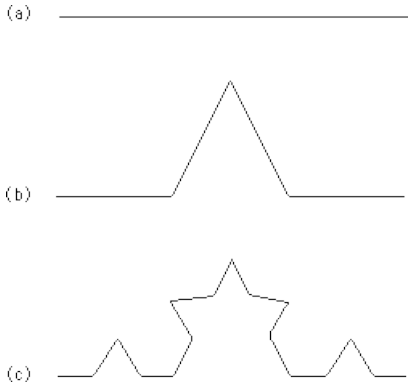

Figure 2.5: Initiator and two steps of the Koch Curve generation process

Then, we iterate the process in each one of the 4 resulting segments. Iterating this process, at the limit, we obtain Koch's Curve (Figure 2.6).

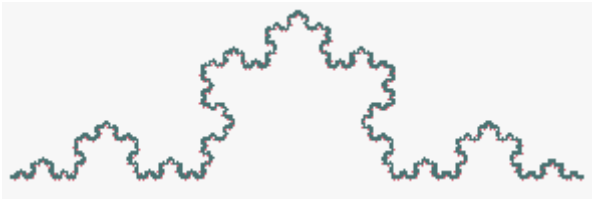

Figure 2.6: Limit of the iteration: Koch's curve

This curve has several, apparently counter intuitive properties, for example, its length is infinite. Like in Mandelbrot's coastline example! Could we use the same method to measure it?

Its infinite is easy to demonstrate: each iteration adds a third of the initial length. So if the segment's length was 1 to begin with, the resulting figure from the first iteration would be $4 * \frac{1}{3} = \frac{4}{3}$. Each one of these 4 segments shall be divided in 4 more, each of a third of its length. This will result in 16 segments of $\frac{1}{9}$. If we continue iterating, we shall see that after the Nth iteration we will have 4^N segments of $\frac{1}{3^N}$. Then, its length is $l(N) = \frac{4^N}{3^N}$. At the limit,

$$\lim_{N \to \infty} \frac{4^N}{3^N} = \infty$$

Joining three curves, we can make the Koch Snowflake (Figure 2.7).

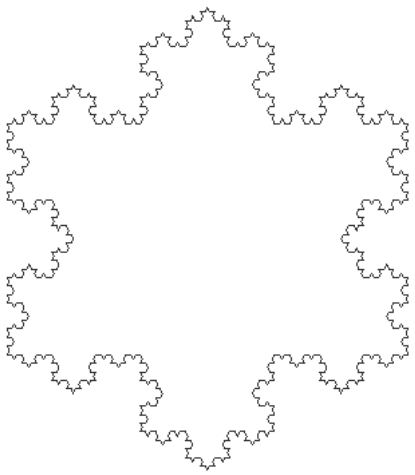

Figure 2.7: Koch Snowflake

2.3 The middle third's Cantor Set.

As in the previous example, we shall take as initiator the segment of a line with the length of 1, and now, as generator, the result of eliminating the middle third of the line (this time adding nothing). The Cantor Set (Figure 2.8) results from iterating the following procedure: for each segment of the line,

we eliminate its middle third, leaving the end points (eliminating the open interval).

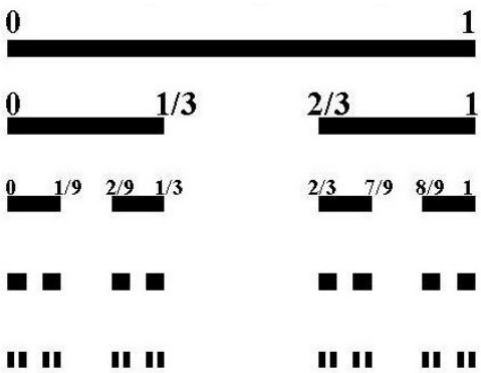

Figure 2.8: Cantor set

Some of the outstanding properties of the Cantor set are that it has no length (or zero length) and that as a set it has a one to one correspondence (bijection) with the initial set, and therefore also with the real numbers. In addition, it is, obviously, self-similar (Figure 2.9).

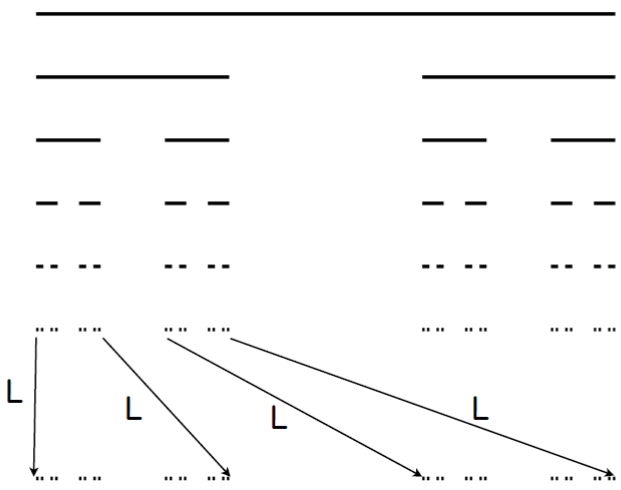

Figure 2.9: The Cantor Set is self-similarity

2.4 Fractal Trees

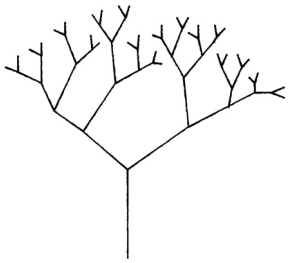

Figure 2.10: Example of a Fractal Tree

In the example in Figure 2.10, we shall look at a tree branching structure. We can see in this figure the tree has a single root with two branches connected at its end. Each branch, in turn, has two branches at its end, and those branches have two branches, and so on. In short, any branch of the tree has the same structure as the whole, and is, therefore, self-similar (Figure 2.11).

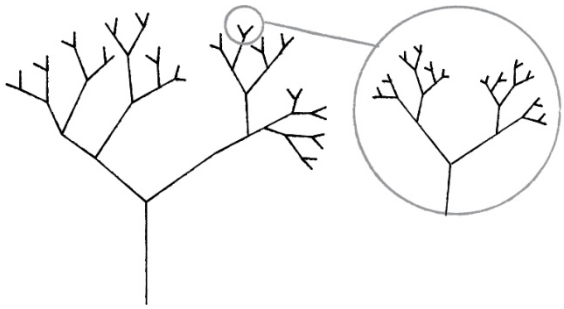

Figure 2.11: Self-similarity of a Fractal Tree

We will now see two examples of fractal trees generated by our own code. The first uses only one drawing pattern and is completely symmetrical in its branches.

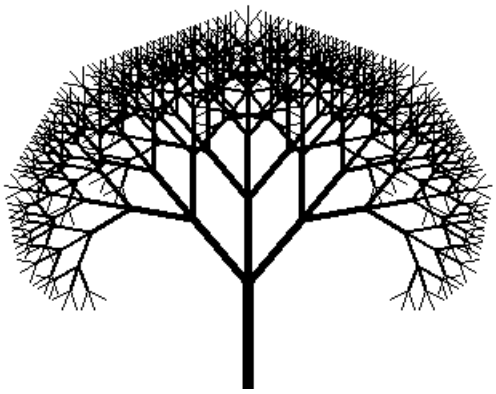

Figure 2.12: Original Symmetric Fractal Tree

The following tree uses a random factor for the size of the branches, which gives it a more realistic appearance.

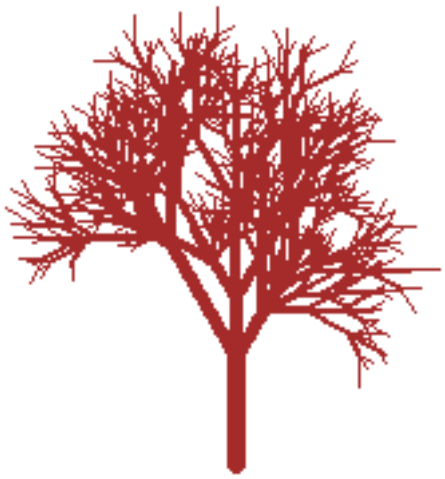

Figure 2.13: Original Random Fractal Tree

3 Geometry of Plane Transformations

In this section, will we show how fractals are generated using plane transformations.

In order to do so, we will first briefly review the features of plane transformations - scaling, reflections, rotations and translations. Afterwards we will show how they are encoded in software, and give some examples.

Note: The images in this chapter come from [5].

3.1 Scaling and reflections

A scaling is a transformation on the plane which, given two factors we will denote r and s, reduces (or augments) the size of the figure to which it is applied. "r" will be the factor for the x axis, and "s" for the y axis.

- If $r = s > 0$ the transformation is a **similarity**.

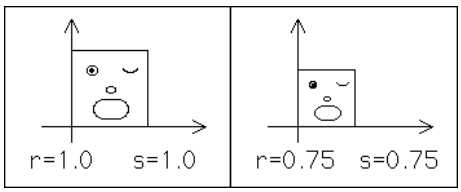

Figure 3.1: Similarity with $r = 0.75$ and $s = 0.75$

- If $r \neq s$ and $r, s > 0$ the transformation is an **affinity**

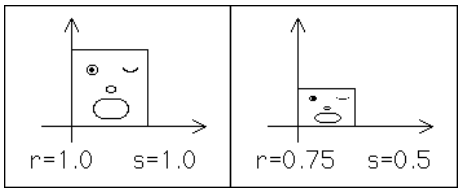

Figure 3.2: Affinity with $r = 0.75$ and $s = 0.5$

- If $r < 0$ and/or $s < 0$ the transformation is a **symmetry**.

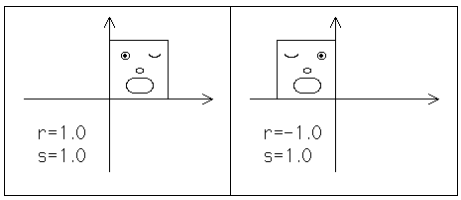

Figure 3.3: Symmetry on the y axis: $r < 0$ and $s > 0$

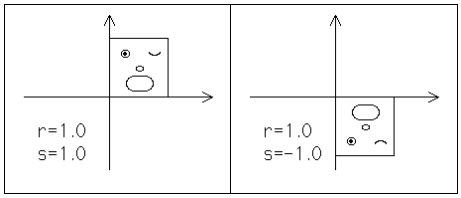

Figure 3.4: Symmetry on the x axis: $r > 0$ and $s < 0$

- Finally, a reflection across both the x- and y-axes is equivalent to rotation by 180° about the origin.

3.2 Rotations

Although it is most common to rotate the entire figure in relation to a certain angle, a rotation is defined by 2 angles we will denominate 'θ' and 'φ', which will indicate the rotation of the horizontal and vertical lines, respectively.

- For example, we may rotate the horizontal lines only, leaving the verticals untouched.

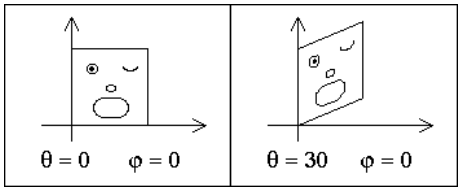

Figure 3.5: Horizontal rotation with $\theta = 0^{\underline{o}}$.

- Or, we can maintain the horizontals and rotate the verticals.

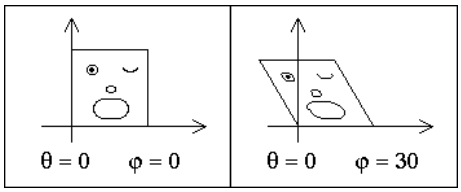

Figure 3.6: Vertical rotation with $\varphi = 30^{\underline{o}}$.

- Finally, if both angles are the same, we rotate in relation to a point, which is the zero of the axes.

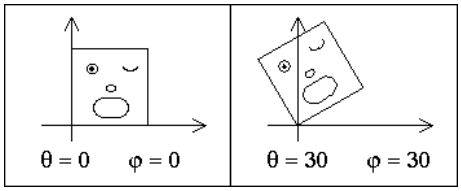

Figure 3.7: Rotation in relation to a point with $\theta = \varphi = 30^{\underline{o}}$.

3.3 Translations

Translations move the entire figure in the plane. We use the variables 'e' and 'f' to refer to the movement realizes on the axes. 'e' for the horizontal axis, and 'f' for the vertical.

- Thus, 'e' moves on the x axis

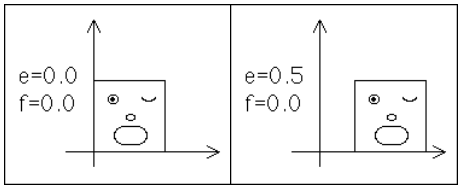

Figure 3.8: Translation on the x axis with e=0.5

- And the same vertically, 'f' moves the figure on the y axis

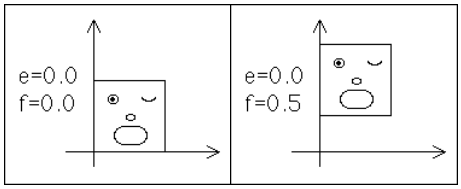

Figure 3.9: Translation on the y axis with f=0.5

3.4 The deterministic algorithm. The matrix formulation

The process of iterating the plane transformations we have previously seen constitutes a deterministic algorithm for the generation of fractals. In the next chapter we will see the general requirements for a set of applications that comprise a deterministic algorithm.

We will now see the matrix formulation of these transformations.

This is the matrix formulation for the transformation that involves scaling by 'r' in the x-direction, by 's' in the y-direction, rotations by 'θ' and 'φ', and translations by 'e' and 'f'.

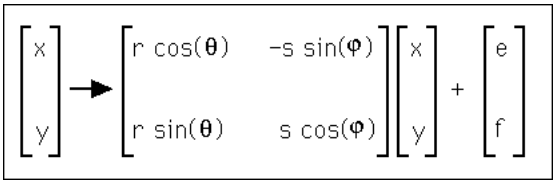

Figure 3.10: The matrix formulation

The order of these transformation is important. For example, reflecting then translating can give a different result from translating then reflecting, as in this next example:

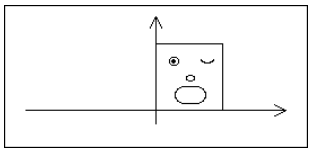

Figure 3.11: Starting picture

Reflection, then translation gives

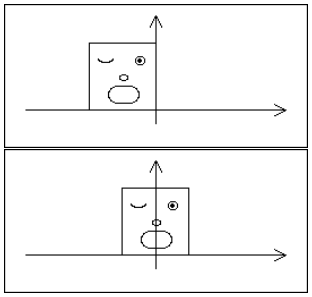

Figure 3.12: Reflection ($r = -1$) and translation ($e = 1/2$).

Translation, then reflection gives

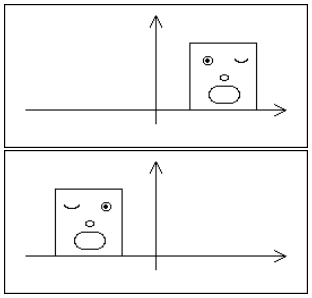

Figure 3.13: Translation ($e = 1/2$) then reflection ($r = -1$).

We adopt this convention: scalings first, reflections second, rotations third, and translations last. This order is imposed by the matrix formulation.

Emphasizing this order, the components of a transformation are encoded in tables of this form.

r	s	θ	φ	e	f

Figure 3.14: Encoded table

With this encoding of transformations on the plane, we can make fractals using the method called Iterated Function Systems (IFS). We will see it in Chapter 4.

Example 3.1. For the Sierpinski Triangle fractal, the deterministic algorithm consists in three plane transformations which can be seen in Figure 3.15: a scaling (in blue), a scaling and a translation to the right (in red), and a scaling with a upward translation (in green). The corresponding values for the plane transformation variables we have just seen appear in the matrix.

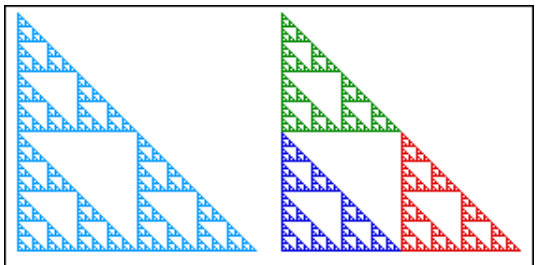

r	s	θ	φ	e	f
0.5	0.5	0	0	0.0	0.0
0.5	0.5	0	0	0.5	0.0
0.5	0.5	0	0	0.0	0.5

Figure 3.15: The matrix encoding for the Sierpinski Triangle

Example 3.2. Here is another fractal, in this case, with a rotation of 90° in the transformation to the right.

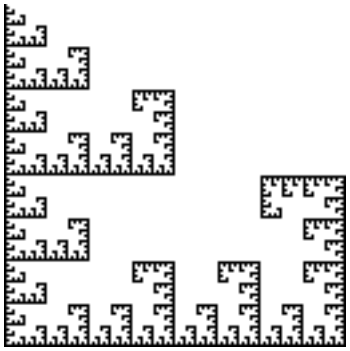

Figure 3.16: A example with rotation (Original generation code).

Example 3.3. Another classic example of fractal construction with plane transformations, the Sierpinski Carpet. In this case, there are 8 transformations based on a scaling of 1/3 and the corresponding translations.

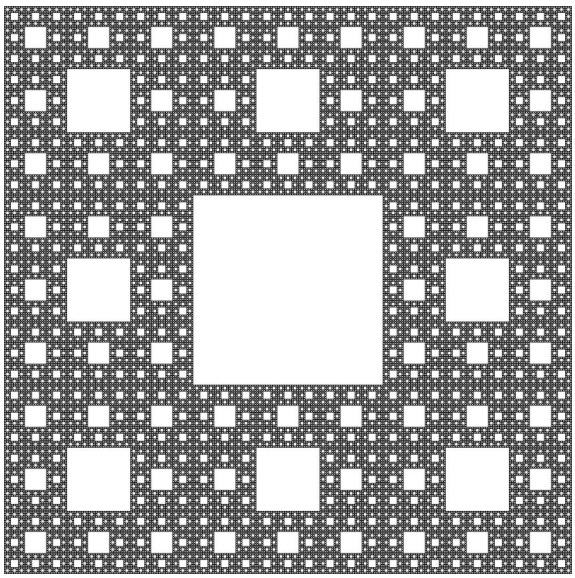

Figure 3.17: Sierpinski Carpet (Original generation code)

4 The Collage Theorem

In this chapter we will present and prove one of the most important theorems in the study of fractals and the theory around them, The Collage Theorem.

It was given by Michael F. Barnsley, with the intention of demonstrating that it is possible to reconstruct images using a set of functions. A digital image can be very big (referring to the amount of memory space it takes up), and a video, with thousands of images, even more so. On the other hand, saving a set of functions may offer a solution to this possible "space¨ problem. This was even more so a few years ago when computers had much less memory capacity then they do now, and made this an important advance in the field.

The Collage Theorem states that we can approximate an image using a IFS (Iterated Function System) with a specific attractor. This will give the desired image regardless of the initial image. To demonstrate this we will use a particular case of the Contraction Mapping Theorem.

4.1 Complete Metric Space

Definition 4.1. A **metric space** is a set X with a global distance function (the metric m) that, for every two points $x, y \in X$, gives the distance between them, $d(x, y)$ as a non-negative real number. For all $x, y, z \in X$, a metric space must also satisfy:

1. Identity of indiscernibles: $d(x, y) = 0 \iff x = y$
2. Symmetry: $d(x, y) = d(y, x)$
3. Triangle inequality: $d(x, y) + d(y, z) \geq d(x, z)$.

Example 4.1. If we let $d(x, y) = |x-y|$, $(\mathbb{R}, d)$ is a metric space. The first two conditions are obviously satisfied, and the third follows from the ordinary triangle inequality for real numbers:

$$d(x, y) = |x-y| = |(x-z) + (z-y)| \leq |x-z| + |z-y| = d(x, z) + d(z, y)$$

Example 4.2. Assume that we want to move from one point $x = (x_1, x_2)$ in the plane to another $y = (y_1, y_2)$, but that we are only allowed to move horizontally and vertically. If we first move horizontally from (x_1, x_2) to (y_1, x_2) and then vertically from (y_1, x_2) to (y_1, y_2), the total distance is $d(x, y) = |y_1 - x_1| + |y_2 - x_2|$. This gives us a metric on $\mathbb{R}^2$ which is different from the usual metric. It is often referred to as the Manhattan Metric (or the taxi cab metric). Also in this case the first two conditions of a metric space are

obviously satisfied. To prove the triangle inequality, observe that for any third point $z = (z_1, z_2)$, we have

$$\begin{aligned} d(x,y) &= |y_1{-}x_1| + |y_2{-}x1| \\ &= |(y_1{-}z_1) + (z_1{-}x_1)| + |(y_2{-}z_2) + (z_2{-}x_2)| \\ &\leq |y_1{-}z_1| + |z_1{-}x_1| + |y_2{-}z_2| + |z_2{-}x_2| \\ &= |z_1{-}x_1| + |z_2{-}x_2| + |y_1{-}z_1| + |y_2{-}z_2| \\ &= d(x,z) + d(z,y) \end{aligned}$$

where we have used the ordinary triangle inequality for real numbers to get from the second to the third line.

Definition 4.2. A sequence $\{a_n\}_n$ is a **Cauchy Sequence** if the metric $d(a_m, a_n)$ satisfies

$$\lim_{\min(m,n)\to\infty} d(a_m, a_n) = 0.$$

See Figure 4.1 for a visual example of a Cauchy and non-Cauchy sequence

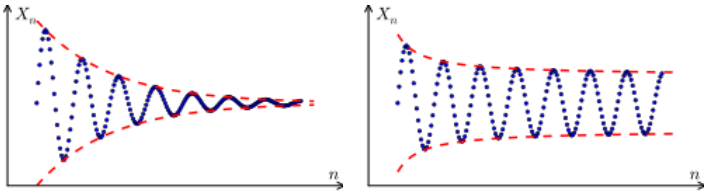

Figure 4.1: Cauchy and non-Cauchy Sequences

Definition 4.3. A sequence S_n **converges** to the limit S, $\lim_{n\to\infty} S_n = S$, if, for any $\epsilon > 0$, there exists an N such that $|S_n - S| < \epsilon$, $\forall n > N$. If S_n does not converge, it is said to **diverge**.

Definition 4.4. A metric space, X, is complete (or a **Complete Metric Space**) if every Cauchy sequence is convergent.

4.2 The Contraction Mapping Theorem

Definition 4.5. A transformation $T : X \to X$ on a metric space (X, d) is called **contractive** or a **contraction mapping** (Figure 4.2) if there is a constant $0 \leq s < 1$ such that $\forall x, y \in X$

$$d(T(x), T(y)) \leq s \cdot d(x, y)$$

Any such number s is called a **contractivity factor** for T.

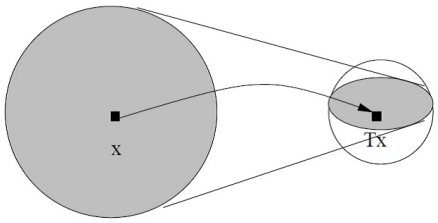

Figure 4.2: Contraction mapping T

Proposition 4.1. *Let $\omega : X \to X$ be a contraction mapping on the metric space (X, d). Then ω is continuous.*

Proof. Let $\epsilon > 0$ be given. Let $s > 0$ be a contraction factor for ω. Then $\forall x, y \in X$

$$d(\omega(x), \omega(\mathrm{y})) \leq \mathrm{s} \cdot d(x, y) < \epsilon$$

whenever $d(x, y) < \delta$, where $\delta = \epsilon / s$. □

Definition 4.6. Let $T : X \to X$ be a transformation on a metric space (X, d). Then, the point $x \in X$ such that $T(x) = x$ is called a fixed point.

With these definitions, we can now give the Contraction Mapping Theorem.

Theorem 4.1. ***(The contraction Mapping Theorem).*** *Let $f : X \to X$ be a contraction mapping on a complete metric space (X, d). Then f possesses exactly one fixed point $x_f \in X$ and moreover for any point $x \in X$, the sequence $\{f^n(x) : n = 0, 1, 2, ...\}$ converges to x_f. That is,*

$$\lim_{n \to \infty} f^n(x) = x_f, \ \ \forall x \in X.$$

Proof. Let $x \in X$. Let $0 \leq s < 1$ be a contractivity factor for f. Then

$$d(f^n(x), f^m(x)) \leq s^{\min(m,n)} d(x, f^{|n-m|}(x))$$

Let $k = |m - n|$. Then,

$$\begin{aligned} d(x, f^k(x)) &\leq d(x, f(x)) + d(f(x), f^2(x)) + ... + d(f^{(k-1)}(x), f^k(x)) \\ &\leq d(x, f(x)) + s{\cdot}d(x, f(x)) + ... + s^{(k-1)}{\cdot}d(x, f(x)) \\ &\leq (1 + s + s^2 + ... + s^{(k-1)})d(x, f(x)) \\ &\leq (1 - s)^{-1}d(x, f(x)), \end{aligned}$$

so substituting into the first equation, we obtain

$$d(f^n(x), f^m(x)) \leq s^{\min(m,n)}(1 - s)^{-1}d(x, f(x))$$

from which it immediately follows that $\{f^n(x)\}_{n=0}^{\infty}$ is a Cauchy sequence. Since X is complete this Cauchy Sequence possesses a limit $x_f \in X$, and we have

$$\lim_{n\to\infty} f^n(x) = x_f$$

Now we shall show that x_f is a fixed point of f, and moreover, that it is unique. By Proposition 4.1 since f is contractive it is continuous, then

$$f(x_f) = f(\lim_{n\to\infty} f(x)) = \lim_{n\to\infty} f^{(n+1)}(x) = x_f$$

Finally, let x_f and y_f be two fixed points of f. Then $x_f = f(x_f), y_f = f(y_f)$, and

$$\begin{aligned} d(x_f, y_f) &= d(f(x_f), f(y_f)) \leq sd(x_f, y_f) \\ &\implies (1 - s)d(x_f, y_f) \leq 0 \\ &\implies d(x_f, y_f) = 0 \end{aligned}$$

And hence, $x_f = y_f$. This complete the proof. □

4.3 The space $\mathcal{K}(X)$. The Hausdorff distance

Definition 4.7. Let (X, d) be a metric space and let $\mathcal{K}(X)$ denote the corresponding **space of non-empty compact subsets of** X.

We need to define a metric for this space.

Definition 4.8. (The Hausdorff distance). Let X, Y be elements of the space $\mathcal{K}$ of non-empty compact subsets of the metric space (X, d). We define

- The distance between $x \in X$ and the compact Y by

$$d(x, Y) := \min_{y\in Y} |x - y|$$

- The distance from the compact X to the compact Y by

$$d(X,Y) := \max_{x \in X}\{d(x,Y)\}$$

Note that this set distance is not symmetric. It has the following properties

1. $B \subset C \implies d(A,C) \leq d(A,B)$
2. $d(A \cup B, C) = \max\{d(A,C), d(B,C)\}$

- **The Hausdorff Distance** d_H between two compacts $X, Y \in \mathcal{K}$ by

$$d_H(X,Y) := \max\{d(X,Y), d(Y,X)\}$$

Remark. In figure 4.3 we can see the Hausdorff distance between two objects in two different positions, which is the radius of the circles.

Hausdorff distance gives a measure of their mutual proximity, by indicating the maximal distance between any point of one polygon to the other polygon, as opposed to the shortest distance (euclidean), which applied only to one point of each polygon, irrespective of all other points of the polygons. As we can see, the Hausdorff distance in both cases is equal to the distance (from one compact to another, as defined above) from the blue triangle to the red one, but bigger than the distance from the red triangle to the blue. We can see that in both figures the euclidean distance is similar and does not consider at all the disposition of the polygons. The Hausdorff distance, however, is sensitive to position, and therefore different in each case.

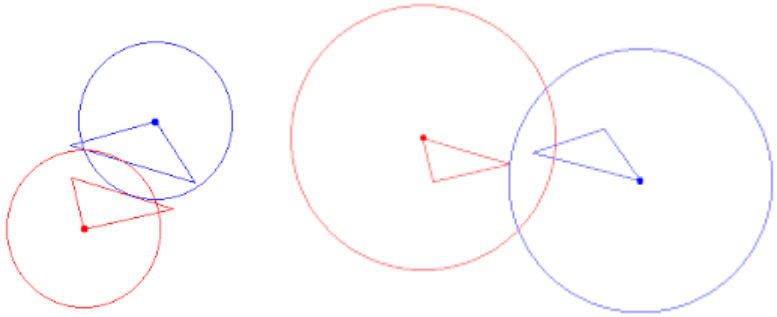

Figure 4.3: Hausdorff distance

Theorem 4.2. *Let (X,d) be a metric space. Then, $(\mathcal{K}(X), d_H)$ denotes a metric space.*

Proof. It is necessary to prove that d_H is a metric in our space $\mathcal{K}(X)$ in order to see that $(\mathcal{K}(X), d_H)$ is a metric space.

Let $A, B, C \in \mathcal{K}(X)$. By definition A, B, C are compact. It is clear that

$$\begin{aligned} h(A,A) &= \max\{d(A,A), d(A,A)\} \\ &= d(A,A) \\ &= \max\{d(x,A) | x \in A\} \\ &= 0 \end{aligned}$$

Let $x \in A, x \notin B$. Then $d(x, B = \inf_{y \in B}\{d(x,y)\} > 0$. Similarly, for $x \in B, x \notin A$. Then $d(x, A = \inf_{y \in A}\{d(x,y)\} > 0$. This implies $d_h(A,B) > 0$, satisfying part (i) of the Definition 4.1.

To show the Triangle Inequality, $d_H(A,B) \leq d_H(A,C) + d_H(C,B)$, we first show it is true for $d(A,B) \leq d(A,C) + d(C,B)$.

For any $x \in A$,

$$\begin{aligned} d(x,B) &= \min_{y \in B}\{d(x,y)\} \\ &\leq \min_{y \in B}\{d(x,z) + d(z,y)\} \forall z \in C\} \\ &= d(x,z) + \min_{y \in B}\{d(z,y)\} \forall z \in C, \text{ so} \\ d(x,B) &\leq \min_{x \in C} d(x,z) + \max_{z \in B}\{\min_{y \in B}\{d(z,y)\}\} \\ &= d(A,B) + d(C,B), \text{ so} \end{aligned}$$

$$d(A,B) \leq d(A,C) + d(C,B)$$

Similarly,

$$d(B,A) \leq d(B,C) + d(C,A)$$

Finally,

$$\begin{aligned} h(A,B) &= \sup\{d(A,B), d(B,A)\} \\ &\leq \sup\{d(B,C), d(C,B)\} + \sup\{d(A,C), d(C,A)\} \\ &= d_H(B,C) + d_H(A,C) \end{aligned}$$

That shows the second and third points, thus d_H is a metric. □

Theorem 4.3. ***(The Completeness of the Space of Fractals)*** *Let (X,d) be a metric space. Then, $(\mathcal{K}(X), d_H)$ is a complete metric space.*

The proof of this theorem exceeds the scope of this paper, Barnsley´s demonstration of it can be found in pg. 36-37 of his his book *Fractals Everywhere[1].*

4.4 Iterated Function Systems. The Collage Theorem

Lemma 4.1. *Let $\omega : X \to X$ be a continuous mapping on the metric space (X, d). Then ω maps $\mathcal{K}$ into itself.*

Proof. Let S be a non-empty compact subset of X. Then clearly $\omega(S) = \{\omega(x) : x \in S\}$ is non-empty. We want to show that $\omega(S)$ is compact. Let $\{y_n = \omega(x_n)\}$ be an infinite sequence of points in S. Then $\{x_n\}$ is an infinite sequence of points in S. Since S is compact there is a subsequence $\{x_{N_n}\}$ that converges to a point $\hat{x} \in S$. But then the continuity of ω implies that $\{y_{N_n}\} = f(x_{N_n})$ is a subsequence of y_{N_n} that converges to $\hat{y} = f(\hat{x}) \in \omega(S)$. And this complete the proof. □

Lemma 4.2. *Let $\omega : X \to X$ be a contraction mapping on the metric space (X, d) with contractivity factor s. Then $\omega : \mathcal{K}(X) \to \mathcal{K}(X)$ defined by*

$$\omega(B) = \{\omega(x) : x \in B\} \ \forall B \in \mathcal{K}(X)$$

is a contraction mapping on $(\mathcal{K}(X), d_H)$ with contractivity factor s.

Proof. From Proposition 4.1 it follows that $\omega : X \to X$ is continuous. Hence by Lemma 4.1 ω maps $\mathcal{K}(X)$ into itself. Now let $B, C \in \mathcal{K}(X)$. Then

$$\begin{aligned} d(\omega(B), \omega(C)) &= \max \min d(\omega(x, y), \omega(y)) : y \in C : x \in B \\ &\leq \max \min s{\cdot}d(x, y) : y \in C : x \in B = s{\cdot}d(B, C). \end{aligned}$$

Similarly, $d(\omega(C), \omega(B)) \leq s{\cdot}d(C, B)$. Hence

$$\begin{aligned} d_H(\omega(B), \omega(C)) &= \max d(\omega(B), \omega(C)), d(\omega(C), \omega(B)) \\ &\leq s \cdot \max\{d(B, C), d(C, B) \\ &\leq s{\cdot}d(B, C) \end{aligned}$$

□

Lemma 4.3. *For all A, B, C, and D, in $\mathcal{K}(X)$*

$$d_H(A \cup B, C \cup D) \leq \max(d_H(A, C), d_H(B, D)),$$

where as usual d_H is the Hausdorff metric.

Proof. Remember that

$$d_H(A \cup B, C \cup D) = max\{d(A \cup B, C \cup D), d(C \cup D, A \cup B)\}$$

Then, we will prove that both are the same.

$$\begin{aligned} d(A \cup B, C \cup D) &= \max\{d(A, C \cup D), d(B, C \cup D)\} \\ &\leq \max\{d(A, C), d(B, D)\} \\ &\leq \max\{\max\{d(A, C), d(C, A)\}, \max\{d(B, D), d\{D, B\}\} \\ &= \max\{d_H(A, C), d_H(B, D) \end{aligned}$$

The same argument yields

$$\begin{aligned} d(C \cup D, A \cup B) &\leq \max\{d(C, A), d(D, B)\} \\ &= \max\{d(A, C), d(B, D)\} \\ &\leq \max\{d_H(A, C), d_H(B, D) \end{aligned}$$

□

Definition 4.9. An **iterated function system** consists of a complete metric space (X, d) together with a finite set of contraction mappings $\omega_n : X \to X$, with respective contractivity factors s_n, for $n = 1, 2, ..., N$. The notation for the IFS just announced is $\{X; \omega_n, n = 1, 2, ..., N\}$ and its contractivity factor is $s = \max\{s_n : n = 1, 2, ..., N\}$.

What an IFS does is scales, translates, and rotates a set using a finite set of functions, which is now possible having demonstrated the Contraction Mapping Theorem.

Example 4.3. Recall our previous example of the Cantor Set (Figure 4.4), and consider the set of functions that generates it. We need two functions, one that scales down by a factor of three, and one that scales and translates by two-thirds the original length. So, we get our IFS $f_1, f-$ where $f_1 = \frac{1}{3}x$ and $f_2 = \frac{1}{3}x + \frac{2}{3}$. As we continue to iterate this function system, we will reach a point where we will not have any intervals, but there will be infinitely many points around a single point, which is the defining property of a Cantor Set.

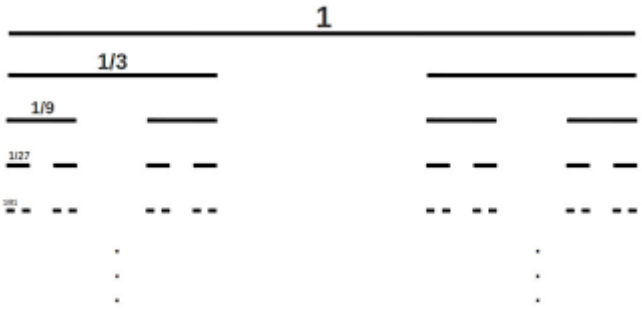

Figure 4.4: Cantor Set

Using notation with IFS,

$$I_1 = f_1(I_0) \cup f_2(I_0)$$

$$I_2 = f_1(I_1) \cup f_2(I_1)$$

...

$$I_n = f_1(I_{n-1}) \cup f_2(I_{n-1})$$

thus,

$$C = f_1(C) \cup f_2(C)$$

where I_0 is the initial interval $[0, 1]$ and C the fixed point of the IFS.

Now we have to show that this fixed point C exists and is unique.

Theorem 4.4. *Let $\{X; \omega_n, n = 1, 2, ..., N\}$ be a iterated function system with contractivity factor s. Then the transformation $W : \mathcal{K}(X) \to \mathcal{K}(X)$ defined by*

$$W(B) = \cup_{n=1}^{N} \omega_n(B)$$

for all $B \in \mathcal{K}(X)$, is a contraction mapping on the complete metric space $(\mathcal{K}(X), d_H)$ with contractivity factor s. That is

$$d_H(W(B), W(C)) \leq s \cdot d_H(B, C)$$

for all $B, C \in \mathcal{K}(X)$.

Proof. For any $B, C \in \mathcal{K}(X)$,

$$\begin{aligned} d_H(W(B), W(C)) &= d_H(\bigcup_{n=1}^{N} \omega_n(B), \bigcup_{n=1}^{N} \omega_n(C)) \\ &\leq^{\text{lema 8}} \max_{n=1}^{N} \{d_H(\omega_n(B), \omega_n(C)\} \\ &=^{def} \max_{n=1}^{N} \{\max\{d(\omega_n(B), \omega_n(C)), d(\omega_n(B), \omega_n(C))\}\} \\ &\leq \max\{s \cdot d(B, C), s \cdot d(C, B)\} \\ &= s \cdot d_H(B, C) \end{aligned}$$

□

Definition 4.10. The transformation W used in the previous theorem is called the **Hutchinson Operator**.

Definition 4.11. An **attractor** is the unique fixed point, $A \in \mathcal{K}(X)$, obeys

$$A = W(A) = \cup_{n=1}^{n} \omega_n(A)$$

and is given by

$$A = \lim_{n \to \infty} W^n(B)$$

for any $B \in \mathcal{K}(X)$.

Corollary 4.1. *Given an Iterated Function System, there exists only one attractor.*

Now that we have a solid background of information about contraction mapping and attractors, we can finally discuss the Collage Theorem, an application of the Banach Fixed-point Theorem.

Theorem 4.5. ***(Collage Theorem for IFS).*** *If $B \in \mathcal{K}(x)$ obeys*

$$d_H(B, W(B)) \leq \epsilon > 0$$

then

$$d_H(B, A) \leq \frac{\epsilon}{(1-s)}$$

where A denotes the attractor of the IFS.

Proof. By the contraction mapping theorem

$$d_H(B, A) = d_H(B, \lim_{n\to\infty} W^n(B)) = \lim_{n\to\infty} d_H(B, W^n B))$$

We will use the induction:
First step: $d_H(B, W(B)) \leq \epsilon < \frac{\epsilon}{(1-s)}$
Now, suppose that $d_H(B, W^n(B)) \leq \frac{\epsilon}{(1-s)}$.
Then we want to show that $d_H(B, W^{n+1}(B)) \leq \frac{\epsilon}{(1-s)}$

$$\begin{aligned} d_H(B, W^{n+1}(B)) &\leq \sum_{m=1}^{n+1} d_H(W^{m-1}(B), W^m(B)) \\ &= \sum_{m=1}^{n+1} d_H(W^{m-1}(B), W^{m-1}(W(B))) \\ &\leq \sum_{m=1}^{n+1} s^{m-1} d_H(B, W(B)) \\ &\leq \frac{1-s^{n+1}}{(1-s)} \cdot \epsilon \\ &\leq \frac{\epsilon}{(1-s)} \end{aligned}$$

And this complete the proof. □

5 The Random Algorithm. The Chaos Game

In the previous chapter we saw the Deterministic Algorithm for fractal generation. Applying some given affine transformations repeatedly to any (compact) initial image, we obtain, at the limit, a fixed point for these transformations. The fixed point will be a fixed image, simultaneously invariable to all the transformations.

In this section we will show another algorithm which serves to represent a fractal, the Chaos Game algorithm. This is one of the best known algorithms that generate a set of points which approximate the attractor sets we have seen in previous sections.

5.1 The algorithm

Let $w_1, \ldots, w_N$ be some norms or applications on a complete metric space X, and $p_1, \ldots p_N$ some nonzero probabilities associated to each one respectively, so that, $\sum_{i=1}^{N} p_i = 1$. These norms are actually contractive function on a complete metric space and therefore constitute an IFS.

The algorithm consists in iterating the following steps:

1. Chose a point $x_0 \in X$.
2. Randomly choose one of the applications w_i according to the probability p_i.
3. Compute the point $x_{n+1} = w_i(x_n)$.
4. Return to step 2 and repeat the process changing x_n for x_{n+1}.

5.2 Example: the Sierpinski Triangle

Let us see, for example, the construction of the Sierpinski Triangle with this algorithm.

Given three points, A, B and C, placed so they are the vertices of an equilateral triangle, we will randomly choose a point x_0 on the plane (even outside the triangle). We will then draw the sequence $x_0, x_1, x_2, \ldots$ created by the following procedure:

- Randomly choose one of the three vertices.
- Draw the middle point between the previous point and the chosen vertex, this will be the next point in the series.
- Repeat the process with the new point.

Let us identify more formally the elements we need in order apply the Chaos Game in the case we have defined:

- The initial point will be a any point (x_0, y_0) in the plane. Supposing we want a triangle with a length of 1 and vertices : $A = (0, 0)$, $B = (1, 0)$, $C = (1/2, \sqrt{3}/2)$.
- The norms shall be :
  - $w_1(x, y) = (x/2, y/2) = ((x, y) + A)/2$
  - $w_2(x, y) = (x/2 + \frac{1}{2}, y/2) = ((x, y) + C)/2$
  - $w_3(x, y) = (x/2 + \frac{1}{4}, y/2 + (3)/4 = ((x, y)C)/2$

In the Figure 5.1 we can see different moments of the process.

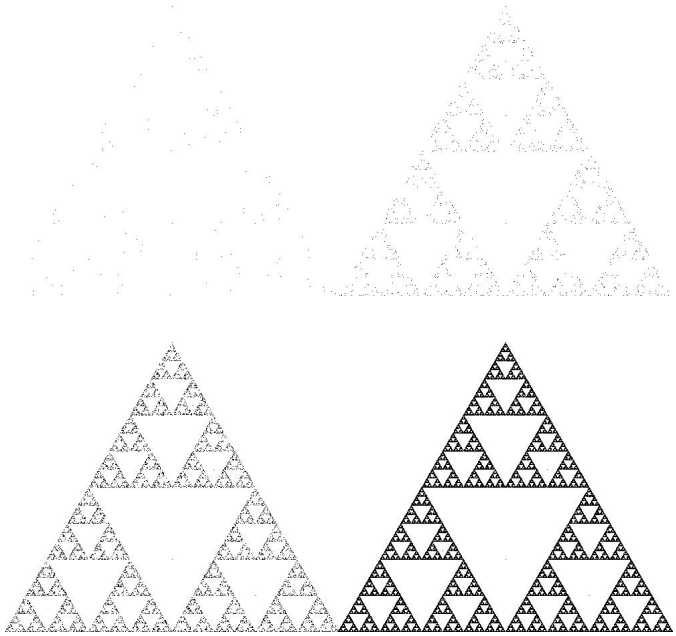

Figure 5.1: The Chaos Game for the Sierpinski Gasket at 100,1.000,10.000 and 100.000.

5.3 Equivalence to the Deterministic Algorithm

As we can see, we have generated the Sierpinski triangle. Or so it seems. But can we really be sure it is the one and same? Can it just be a very similar looking set? And what about the random order in which we applied the functions? Would another order produce a different result? And the initial

point? Does it matter if it is part of the attractor set or would just any point in the plane do? The following theorem will clear all doubts.

Let us quickly remind ourselves of some concepts we discussed earlier:

- An **Iterated Function System** on a complete metric space (X, d) is a finite collection $\{w_1, ..., w_N\}$, $N > 1$, of contractions $w_i : X \to X$ (see Definition 4.9).
- Denote by $\mathcal{K}(X)$ the collection of the non-empty compact subsets of a complete metric space (X, d) and d_H the Hausdorff metric induced by the metric d. $(\mathcal{K}(X), d_H)$ is a metric space (see Section 4.3).
- Given an IFS, we can define the **Hutchinson operator** W as a transformation on the metric space $(\mathcal{K}(X), d_H)$:

$$W(E) = \bigcup_{i=1}^{N} w_i(E) \ , \ E \in \mathcal{K}(X), \tag{5.1}$$

- On the basis of the Collage Theorem (see Theorem 4.5) there is a set $\mathcal{A} \in \mathcal{K}(X)$ that is the unique **fixed point** of W, called the *attractor* of the IFS. Hence,

$$\mathcal{A} = W(\mathcal{A}) \tag{5.2}$$

- Let w_i be a contractive mapping (see Definition 4.5), therefore, we have

$$d(w_i(x), w_i(y)) \leq s_i.d(x, y) \ , \text{ for any } x, y \in X$$

where s_i denotes the contractivity factor of w_i.

Definition 5.1. The **diameter** of a subset $E \subset X$ shall be

$$diam(E) = \sup_{x,y \in E} \{d(x, y)\} \tag{5.3}$$

for any $x, y \in E$.

Theorem 5.1. *Let $\{w_1, ..., w_N\}$ be an IFS on a complete metric space (X, d). Let $\mathcal{A}$ be the attractor of the IFS. Let $\{x_n\}_{n=0}^{\infty}$ be a set of points generated by the Chaos Game, where x_0 is any point of X. Then, with probability 1, for any $\epsilon > 0$, there is a number $M \in \mathbb{N}$ such that $d_H(\mathcal{A}, \overline{\{x_n\}_{n=M}^{\infty}}) \leq \epsilon$. That is, the closure of the set $\{x_n\}_{n=M}^{\infty}$ approximates $\mathcal{A}$ with an error no greater than ϵ with respect to the Hausdorff metric, d_H.*

Proof. The proof consists of two parts. In the first, we assume that the initial point x_0 belongs to the attractor $\mathcal{A}$ and show that the set $\{x_n\}_{n=M}^{\infty}$ is dense in $\mathcal{A}$ for any $M \in \mathbb{N}$ - thus $\overline{\{x_n\}_{n=M}^{\infty}} = A$. Then, in the second part, we use

that fact to show the correctness of the Chaos Game in the more general case in which x_0 is any point of X.

Let $x_0 \in \mathcal{A}$. By (5.1) the IFS mappings transform the attractor into itself, so $\{x_n\}_{n=0}^{\infty} \subset \mathcal{A}$. Let a be any point of $\mathcal{A}$. In order to prove that $\{x_n\}_{n=M}^{\infty}$ is dense in $\mathcal{A}$ for any $M \in \mathbb{N}$, we need to show that for any $\epsilon > 0$ and any $M \in \mathbb{N}$, the subset $\{x_n\}_{n=M}^{\infty}$ includes, with probability 1, a point $x \in \mathcal{A}$ such that $d(x, a) \leq \epsilon$.

On the basis of (5.2) we have

$$\mathcal{A} = W^{ok}(\mathcal{A}) = \bigcup_{i_1,...,i_k \in \{1,...,N\}} w_{i_1}, ..., w_{i_k}, \text{ for any } k \in \mathbb{N}.$$

And, based on (5.3), for any $E \subset X$

$$diam(w_i(E)) = \sup_{x,y \in E} d(w_i(x), w_i(y)) \leq \sup_{x,y \in E} \{s_i.d(x, y)\}$$

The attractor $\mathcal{A}$ can be regarded as a finite union of N^k subsets $w_{i_1} \circ ... \circ w_{i_k}(\mathcal{A})$. The diameter of each subset will depend on k. Let us bind this diameter by an arbitrary ϵ.

$$\begin{aligned} diam(w_{i_1} \circ ... \circ w_{i_k}(\mathcal{A})) \quad \leq \quad & (\max_{i=1,...,N} s_i)^k.diam(\mathcal{A}) \leq \epsilon \\ & \Longrightarrow \log((\max_{i=1,...,N} s_i)^k.diam(\mathcal{A})) \leq \log \epsilon \\ & \Longrightarrow \log((\max_{i=1,...,N} s_i)^k + \log(diam(\mathcal{A}))) \leq \log \epsilon \\ & \Longrightarrow k \cdot \log(\max_{i=1,...,N} s_i) + \log(diam(\mathcal{A}))) \leq \log \epsilon \\ & \Longrightarrow k.\log(\max_{i=1,...,N} s_i) \leq \log \epsilon - \log(diam(\mathcal{A})) \end{aligned}$$

So given $\epsilon > 0$ and as $0 < s_i < 1$, taking

$$k \geq \frac{\log \epsilon - \log(diam(\mathcal{A}))}{\log(\max_{i=1,...,N} s_i)}$$

we have

$$diam(w_{i_1} \circ ... \circ w_{i_k}(\mathcal{A})) \leq \epsilon$$

Hence, the point a belongs to at least one of the sets of the attractor decomposition, say $a \in w_{i_1} \circ ... \circ w_{i_k}(\mathcal{A})$. Thus, if, starting from any mth iteration of the Chaos Game, the sequence $w_{i_k}, ..., w_{i_1}$ of the IFS mappings gets chosen in the k successive iterations of the algorithm, then the point $x_{m+k-1} \in \{x_n\}_{n=0}^{\infty}$ will belong to the set $w_{i_1} \circ ... \circ w_{i_k}(\mathcal{A})$ and, hence, $d(x_{m+k-1}, a) \leq \epsilon$. Now we will show that, with probability 1, the sequence will occur infinitely many times as the Chaos Game proceeds.

Let B_m denote the event that the mappings $w_{i_k}, ..., w_{i_1}$ get chosen successively in the mth,$(m+1)$th,...,$(m+k-1)$th iteration of the Chaos Game respectively. Since, in successive iterations of the algorithm the IFS mappings are chosen independently, the probability for the event B_m to occur is

$$P(B_m) = \prod_{j=1}^{k} p_{i_j} > 0 \tag{5.4}$$

Obviously the events B_m, $m = 1, 2, ...$, are not independent. Nevertheless, the events B_{km}, $m = 1, 2, ...$, are independent and, thus, the occurrence of the events from the subsequence $\{B_{km}\}_{m=1}^{\infty}$ can be regarded in terms of infinite Bernoulli trials with probabilities p for success specified by (5.4). On the basis of Borel's law of large numbers [3] we have that with probability 1,

$$\lim_{m\to\infty} \frac{S_m}{m} = p$$

where S_m denotes the number of successes in the first m trials. Hence, with probability 1, $S_m \to \infty$ as $m \to \infty$. Therefore, during the infinite iteration of the Chaos Game, infinitely any events from the subsequence $\{B_{km}\}_{m=1}^{\infty}$ will occur, and all the more so from the sequence $\{B_m\}_{m=1}^{\infty}$.

On the basis of the above, for any $M \in \mathbb{N}$, during the infinite iteration of the Chaos Game, infinitely many events from $\{B_m\}_{m=M}^{\infty}$ will occur with probability 1 as well. The point a has been specified as any point of the attractor $\mathcal{A}$. Therefore, assuming that the initial point $x_0 \in \mathcal{A}$, it follows that, with probability 1, the set $\{B_m\}_{m=M}^{\infty}$ is dense in A.

Now we go to the second part of the proof in which we will take the initial point x_0 to be any point of the space X. Let $\{x_n\}_{n=0}^{\infty}$ and $\{y_n\}_{n=0}^{\infty}$ be the sets of points which are generated concurrently by the same realization of the Chaos Game for the initial points $x_0 \in X$ and $y_0 \in \mathcal{A}$, respectively. In other words, $x_{n+1} = w_i(x_n)$ and $y_{n+1} = w_i(y_n)$, where w_i is the IFS mapping chosen in the mth iteration of the algorithm. Since the IFS mappings are contractive, we obtain that the distance between the points x_n and y_n in the mth iteration satisfies

$$\begin{aligned} d(x_m, y_m) &= d(w_{i_m} \circ ... \circ w_{i_1}(x_0), w_{i_m} \circ ... \circ w_{i_1}(y_0)) \\ &\leq \prod_{j=1}^{m} s_{i_j} d(x_0, y_0) \end{aligned}$$

and, moreover, for any $n > m$,

$$d(x_n, y_n) \leq s^{n-m} d(x_m, y_m),$$

where $s = \max_{i=1,...,N} s_i < 1$. It follows that for any $\epsilon > 0$, there is an $M \in \mathbb{N}$ such that the distance $d(x_n, y_n) \leq \epsilon$ for every $n \geq M$. Hence, the

Hausdorff distance between the closures of the subsets $\{x_n\}_{n=M}^{\infty}$ and $\{y_n\}_{n=M}^{\infty}$ satisfies

$$d_H(\overline{\{x_n\}_{n=M}^{\infty}}, \overline{\{y_n\}_{n=M}^{\infty}}) \leq \epsilon.$$

But $y_0 \in \mathcal{A}$. So on the basis of the first part of the proof, $\overline{\{y_n\}_{n=M}^{\infty}} = \mathcal{A}$ with probability 1. This completes the proof. □

We can now assert that the Chaos Game generates a sequence of points which, at its closure is the attractor of the IFS or, in the case of an initial point which is not in the attractor, a sequence of points which comes infinitely close to the attractor, and its closure arbitrarily close to it. Furthermore, we have seen that neither the order in which we select the functions, nor the initial point chosen, effect the result (in the same way the initial compact does not effect the resulting attractor in the deterministic algorithm).

Thus, we finalize this chapter with the conclusion that the random algorithm and the deterministic one are equivalent to each other.

6 Fractal dimensions

In previous chapters we have presented the idea of fractals, and seen some examples. We have also explained some concepts necessary for their generation and were able to enunciate formally the two basic and equivalent algorithms that generate them – the deterministic and the random one.

We will now go on to study an important property of fractals - the Fractal Dimension. This property is so important that it is often used to define a fractal, as a set who´s fractal dimension is greater the the topological one. Falconer considers [4] this definition unsatisfactory in that it excludes a number of sets that ought to be regarded as fractals. Nonetheless this property has many practical applications for the study of natural phenomena which will see in the last chapter of this paper.

6.1 The topological dimension

The common notion of dimension is that which is called the topological dimension, and it is always a natural number.

All the fractals we have seen can be represented on a plane, so their dimension should be no greater than 2. Let us take as an example Koch's Curve, which we have seen earlier (Figure 2.6).

At a glance, we can say the dimension is 1. And why not? It is obviously more then 0 since it is not a totally disconnected set of isolated points. On the other hand, it does not have an area, so its dimension must be less than 2. So the topological dimension of the curve is 1.

But this seems insufficient, since the curve is very dense. Its length is infinite within a closed space.

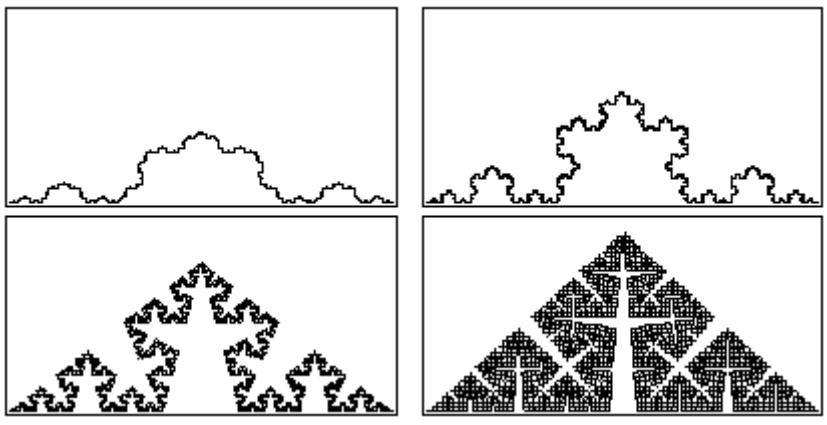

Figure 6.1: Curves of different densities.

Could we find a way to quantify the density of each fractal in figure 6.1. Could we distinguish by this density a piece of coastline of two different countries without seeing the entire country? Or, could we tell apart a healthy heart

from a sick one by just looking at an image of a small part of it. How about the other way around, generating an image of a forest knowing only the structure of one tree.

In order to do so, and much more, we would require a new dimension that will enable us to compare fractals.

This dimension represents an idea of how densely a fractal occupies the metric space in which it is found, and enable us to make comparisons between different fractals.

As we will see, various definitions of fractal dimension exist. Lets us see the most general case, which is the Hausdorff Dimension, and some particular cases of it, which are specific dimensions for simpler fractals.

6.2 The Hausdorff measure and dimension

The Hausdorff measure

Definition 6.1. Let E be a non-empty subset of n-dimensional Euclidean space, $\mathbb{R}^n$. A δ-cover of the subset E is a countable (or finite) collection of sets, which each have a diameter of at most δ, and which cover E, i.e. $E \subset \bigcup_{i=1}^{\infty} U_i$ with $0 \leq diam(U_i) \leq \delta$ for each i.

Definition 6.2. Let E be a non-empty subset of $\mathbb{R}^n$,$\{U_i\}$ a δ-cover of E, and s a non-negative number. For any $\delta > 0$ we define

$$\mathcal{H}^s_\delta(E) := \inf \left\{ \sum_i^{\infty} diam(U_i)^s \right\}$$

Thus we look at all covers of E by sets of diameter at most δ and seek to minimize the sum of the sth powers of the diameters. As δ decreases, the class of permissible covers of E is reduced. Therefore, the infimum $\mathcal{H}^s_\delta(E)$ increases, and so approaches a limit as $\delta \to 0$.

Definition 6.3. Let E be a non-empty subset of $\mathbb{R}^n$. We define the s-dimensional Hausdorff measure of E as

$$\mathcal{H}^s(E) = \lim_{\delta \to \infty} \mathcal{H}^s_\delta(E)$$

Observe that this limit exists for any subset E, thought the limiting value can be (and usually is) 0 or ∞.

with a certain amount of effort, $\mathcal{H}^s(E)$ may be shown to be a measure, and $(\mathbb{R}^n, \mathcal{H}^s(E))$ a metric space. The in-depth exploration of measurements is beyond the scope of this paper, these demonstrations can be found in the book *Fractal geometry*[4].

The Hausdorff-Besicovitch dimension

Based on the Definition 6.2 it is clear that for any given set $E \subset \mathbb{R}^n$ and $\delta < 1$, $\mathcal{H}^s_\delta(E)$ is non-increasing with s, so, by Definition 6.3, $\mathcal{H}^s(E)$ is also non-increasing. In fact, rather more is true: if $t > s$ and $\{U_i\}$ is a δ-cover of E we have

$$\sum_i diam(U_i)^t \leq \sum_i diam(U_i)^{t-s} diam(U_i)^s \leq \delta^{t-s} \sum_i diam(U_i)^s$$

so, taking infima, $\mathcal{H}^t_\delta(E) \leq \delta^{t-s}\mathcal{H}^s_\delta(E)$. Letting $\delta \to 0$ we see that if $\mathcal{H}^s(E) < \infty$ then $\mathcal{H}^t(E) = 0$ for $t > s$. Thus a graph of $\mathcal{H}^s(E)$ against s shows that there is a critical value of s at which $\mathcal{H}^s(E)$ 'jumps' from ∞ to 0 (see Figure 6.2). This critical value is called the **Hausdorff dimension** of E; it is defined for any set $E \subset \mathbb{R}^n$. Formally

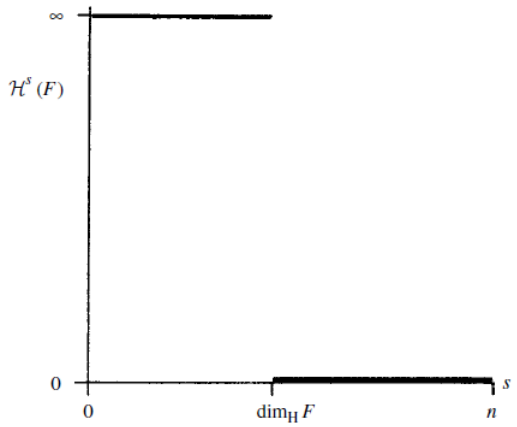

Figure 6.2: Graph of $\mathcal{H}^s(E)$ against s

Definition 6.4. Let E be a non-empty subset of $\mathbb{R}^n$. Let $\mathcal{H}^s(E)$ be the s-dimensional Hausdorff measure of E. The Hausdorff dimension of E is

$$dim_H F = \inf\{s \geq 0 : \mathcal{H}^s(E) = 0\} = \sup\{s : \mathcal{H}^s(E) = \infty\}.$$

so that

$$\mathcal{H}^s(E) = \begin{cases} \infty & \text{if } 0 \leq s < dim_H E \\ 0 & \text{if } s > dim_H E \end{cases}$$

Hausdorff measures generalize the familiar ideas of length, area, volume, etc. It may be shown that, for subsets of $\mathbb{R}^n$, n-dimensional Hausdorff measure

is, with a constant multiple, just n-dimensional Lebesgue measure, i.e. the usual n-dimensional volume. More precisely, if E is a Borel subset of $\mathbb{R}^n$, then

$$\mathcal{H}^n(E) = c_n^{-1} vol^n(E)$$

where c_n is the volume of an n-dimensional ball of diameter 1, so that $c_n = \pi^{n/2}/2^n(n/2)!$ if n is even and $c_n = \pi^{(n-1)/2}((n-1)/2)!/n!$ if n is odd. Similarly, for 'nice' lower-dimensional subsets of $\mathbb{R}^n$, we have that $\mathcal{H}^0(E)$ is the number of points in E; $\mathcal{H}^1(E)$ gives the length of a smooth curve E; $\mathcal{H}^2(E) = (4/\pi) \cdot Area(E)$ if E is a smooth surface; $\mathcal{H}^3(E) = (6/\pi) \cdot vol(E)$; and $\mathcal{H}^m(E) = c_m^{-1} vol^m(E)$ is a smooth m-dimensional submanifold of $\mathbb{R}^n$ (i.e. an m-dimensional surface in the classical sense).

Example. For a very simple example, let E be a flat disc of unit radius in $\mathbb{R}^3$. From familiar properties of length, area and volume, $\mathcal{H}^1(E) = length(E) = \infty$, $0 < \mathcal{H}^2(E) = (4/\pi) \cdot area(E) = 4 < \infty$ and $\mathcal{H}^3(E) = (6/\pi) \cdot vol(F) = 0$. Thus $dim_H E = 2$, with

$$\mathcal{H}^s(E) = \begin{cases} \infty & \text{if } s < 2 \\ 0 & \text{if } s > 2 \end{cases}$$

The Hausdorff dimension, in general, is complicated to compute. But for particular cases, such as self-similar fractals this complication can be significantly reduced. In the next section we will see how to easily calculate their dimension.

The Self-similarity Dimension

Most of the objects we have seen in this paper, and the simplest in terms of fractal geometry, are those generated by affinities with the same contraction factor. That is to say, strictly self-similar objects, made by scaled down, exact copies of themselves.

The scaling properties of length, area and volume are well known. On magnification by a factor λ, the length of a curve is multiplied by λ, the area of a plane region is multiplied by λ^2 and the volume of a 3-dimensional object is multiplied by λ^3. As might be anticipated, s-dimensional Hausdorff measure scales with a factor λ^s (see Figure 6.3).

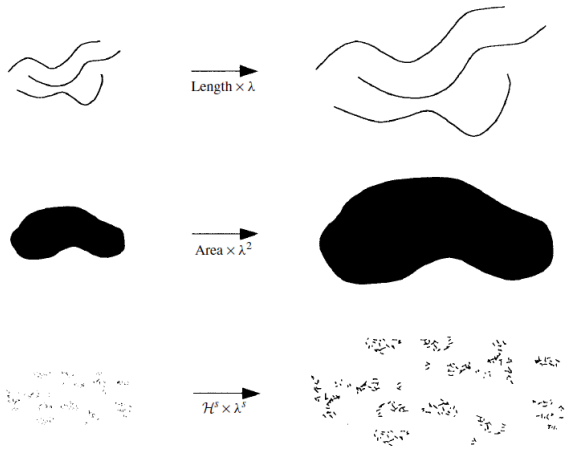

Figure 6.3: Scaling sets by a factor λ increases length by a factor λ, area by a factorλ^2, and s-dimensional Hausdorff measure by a factorλ^s.

Proposition 6.1. (**Scaling property**). *Let S be a similarity transformation of scale factor $\lambda > 0$. If $E \subset \mathbb{R}^n$, then*

$$\mathcal{H}^s(S(E)) = \lambda^s \mathcal{H}^s(E).$$

Proof. If $\{U_i\}$ is a δ-cover of E then $\{S(U_i)\}$ is a $\lambda\delta$-cover of $S(E)$, so

$$\sum diam(S(U_i))^s = \lambda^s \sum diam(U_i)^s$$

so

$$\mathcal{H}^s_{\lambda\delta}(S(E)) \leq \lambda^S \mathcal{H}^s_\delta(E)$$

on taking the infimum. Letting $\delta \to 0$ gives that $\mathcal{H}^s(S(E)) \leq \lambda^S \mathcal{H}^s(E)$. Replacing S by S^{-1}, and so λ by $1/\lambda$, and E by $S(E)$ gives the opposite inequality required. This complete the proof. □

We will see how to calculate the Hausdorff Dimension of a Self-similarity fractal with the Middle third's Cantor Set example.

Example. Let E be the Middle Third Cantor Set (Figure 2.8). If $s = \log(2)/\log(3)$, then $dim_H E$=s and $1/2 \leq \mathcal{H}^s(E) \leq 1$.

Heuristic calculation. The Cantor Set E splits a left part $E_L = E \cap [0, \frac{1}{3}]$ and a right part $E_R = E \cap [\frac{2}{3}, 1]$. Clearly both parts are geometrically similar to E but scaled by a ratio $\frac{1}{3}$, and $E = E_L \cup E_R$ with this union disjoint. Thus for any s

$$\mathcal{H}^s(E) = \mathcal{H}^s(E_L) + \mathcal{H}^s(E_R) = (\frac{1}{3})^s \mathcal{H}^s(E) + (\frac{1}{3})^s \mathcal{H}^s(E) = 2(\frac{1}{3})^s \mathcal{H}^s(E)$$

by the scaling property (Proposition 6.1) of Hausdorff measures. Assuming that at the critical value $s = dim_H E$ we have $0 < \mathcal{H}^s(E) < \infty$ (a big assumption, but one that can be justified) we may divide by $\mathcal{H}^s(E)$ to get $1 = 2(\frac{1}{3})^s$ or $s = \log(2)/\log(3)$.

Rigorous calculation. We call the intervals that make up the sets E_k in the construction of E level-k intervals. Thus E_k consists of 2^k level-k intervals each of length 3^{-k}.

Taking the intervals of E_k as a 3^{-k} cover of E gives that $\mathcal{H}^s_{3^{-k}}(E) \leq 2^k 3^{-ks} = 1$ if $s = \log(2)/\log(3)$. Letting $k \to \infty$ gives $\mathcal{H}^s(E) \leq 1$.

To prove that $\mathcal{H}^s(E) \geq \frac{1}{2}$ we show that

$$\sum diam(U_i)^s \geq \frac{1}{2} = 3^{-s} \tag{6.1}$$

for any cover $\{U_i\}$ of E. Clearly, it is enough to assume that the $\{U_i\}$ are intervals, and by expanding them slightly and using the compactness of E, we need only verify (6.1) if $\{U_i\}$ is a finite collection of closed subintervals of $[0, 1]$. For each U_i, let k be the integer such that

$$3^{-(k+1)} \leq diam(U_i) < 3^{-k}. \tag{6.2}$$

Then U_i can intersect at most one level-k interval since the separation of these level-k intervals is at least 3^{-k}. If $j \geq k$ then, by construction, U_i intersects at most $2^{j-k} = 2^j 3^{-sk} \leq 2^j 3^s diam(U_i)^s$ level-j intervals of E_j, using (6.2) if we choose j large enough so that $3^{-(j+1)} \leq diam(U_i)$ for all U_i, then since the $\{U_i\}$ intersect all 2^j basic intervals of length 3^{-j}, counting intervals gives $2^j \leq \sum_i 2^j 3^s diam(U_i)^s$, which reduces to (6.1).

With extra effort, the calculation can be adapted to show that $\mathcal{H}^s(E) = 1$. That is to say the s-dimensional Hausdorff measure is 1, with $s = \log(2)/\log(3)$.

6.3 The Box-counting dimension

Box-counting dimension is one of the most widely used dimensions. Its popularity is largely due to its relative ease of mathematical calculation and empirical estimation.

Definition 6.5. Let E be any non-empty bounded subset of $\mathbb{R}^n$ and let $N_\delta(E)$ be the smallest number of sets of diameter at most δ which can cover E. The ***lower*** and ***upper box-counting dimension*** of E respectively are defined as

$$\underline{dim}_B E = \underline{\lim}_{\delta \to 0} \frac{\log N_\delta(E)}{-\log \delta}$$

$$\overline{dim}_B E = \overline{\lim}_{\delta \to 0} \frac{\log N_\delta(E)}{-\log \delta}$$

If these are equal we refer to the common value as the **box-counting dimension** of E

$$dim_B E = \lim_{\delta \to 0} \frac{\log N_\delta(E)}{-\log \delta}$$

we can see that considering subset E as non-empty and bounded, we avoid problems with $\log 0$ y $\log \infty$.

There are several equivalent definitions of box-counting dimension that are sometimes more convenient to use. We shall explain one of those. Consider the collection of cubes in the δ-coordinate mesh of $\mathbb{R}^n$, i.e. cubes of the form

$$[m_1\delta, (m_1+1)\delta] \times \cdots \times [m_n\delta, (m_n+1)\delta]$$

where $m_1, ..., m_n$ are integers. Let $N'_\delta(E)$ be the number of δ-mesh cubes that intersect E. They obviously provide a collection of $N'_\delta(E)$ sets of diameter $\delta\sqrt{n}$ that cover E, so

$$N_{\delta\sqrt{n}}(E) \leq N'_\delta(E).$$

If $\delta\sqrt{n} < 1$ then

$$\frac{\log N_{\delta\sqrt{n}}(E)}{-\log \delta\sqrt{n}} \leq \frac{\log N'_\delta(E).}{-\log \sqrt{n} - \log \delta}$$

so taking limits as $\delta \to 0$

$$\underline{dim}_B E \leq \underline{\lim}_{\delta \to 0} \frac{\log N'_\delta(E)}{-\log \delta}$$

$$\overline{dim}_B E \leq \overline{\lim}_{\delta \to 0} \frac{\log N'_\delta(E)}{-\log \delta}$$

On the other hand, any set of diameter at most δ is contained in 3^n mesh cubes of side δ. Thus

$$N'_\delta(E) \leq 3^n N_\delta(E)$$

and taking logarithms and limits as $\delta \to 0$ leads to the opposite inequalities. Hence to find the box-counting dimensions we can equally well take $N_\delta(E)$ to be the number of mesh cubes of side δ that intersect E.

This version of the definitions is widely used empirically. To find the box dimension of a plane set E we draw a mesh of squares or boxes of side δ. The dimension is the logarithmic rate at which $N_\delta(E)$ increases as $\delta \to 0$, and may be estimated by the gradient of the graph of $\log N_\delta(E)$ against $-\log \delta = \log(1/\delta)$.

6.4 Box-counting calculating program

We will now present an original program, written in Python, which calculates the box-counting dimension for any image, using the equivalent version we have just described.

```
from PIL import Image
import math

im = Image.open('fractal.jpg')#open any image

sizex = im.size[0]
sizey = im.size[1]

m1 = 32 #size of first mesh cube
m2 = 64 #size of first mesh cube

#Compute MCD and mcm
A = max(m1, m2)
B = min(m1, m2)
while B:
        mcd = B
        B = A % B
        A = mcd
mcm =  (m1 * m2) // mcd

perfectSize = 0
while perfectSize<sizex:
        perfectSize += mcm

#this function converts the color information in binary
def negre(m,mx,my,x,y):
        for i in range(m*x,m*x+mx):
                for j in range(m*y,m*y+my):
                        if im.getpixel((i,sizex-1-j))[0] < 230:
                                return 1
        return 0

#this function counts how many of the mesh cube regions intersect with
def calCount(m):
        dimx = perfectSize/m
        dimy = perfectSize/m
        count = 0
        i = 0
        while (i+1)*m < sizex:
                j = 0
                while (j+1)*m < sizey:
                        if negre(m,m,m,i,j) == 1:
                                count = count +1
                        j += 1
```

```
            if negre(m,m,sizey-j*m,i,j):
                    count = count +1
            i = i+1
    j = 0
    print "ultima columna"
    while (j+1)*m < sizey:
            if negre(m,sizex-i*m,m,i,j):
                    count = count + 1
            j += 1
    print "ultim quadrat dalt dreta"
    if negre(m,sizex-i*m,sizey-j*m,i,j):
            count = count + 1
    return count

boxDimNum = (math.log(calCount(m1))-math.log(calCount(m2)))
boxDimDen = (math.log(float(1)/m1)-math.log(float(1)/m2))
boxDime = boxDimNum / boxDimDen #the box-counting dimension
```

Although theoretically sound, the program meets with some practical limitations. Any image can be analyzed, but some give a significant error. This is due to the limitation of images constructed of pixels, which must be either "full" or "empty", where the fractal form should actually continue. Best results are achieved with self-similar fractals, due to their simplicity. Here are some examples.

7 Applications

So, having studied fractals, their construction, properties and dimensions, can we now answer Mandelbrot´s question – "how long is the coast of Britain?". Actually, we can´t. It´s a paradox. The length of the coastline depends on scale, the closer we get, the longer it measures. The coast of Spain, for example, is 4.964 km according to The World Factbook; 7.268 km according to the WRI; and 7.879 km according to IGN (there is no international agreement on the scale of measurement).

We can see that the property of length, which is clear cut in perfect geometric objects, is not so for a coastline. If we had an infinitely fine ruler, atomically fine, the coastline of any country would be very long indeed. The question of length in natural, rough, objects becomes senseless. Like a 1:1 map of the world proposed by Lewis Carroll, it affords no useful information and only blocks the sunlight.

We can, on the other hand, know some useful numbers about coastlines, or any other fractal-like object: there is a stable ratio between the change in scale and the change in detail, which is the fractal dimension. This dimension gives us information about the world and, as we have said, has many practical applications. Let us see some examples:

7.1 Coronary dysfunctions

Many studies have been made about the use of fractal dimensions in the service of medicine. Arterial and venous trees and the branching of certain cardiac muscle bundles and a number of complex anatomic structures display fractal-like geometry. These self-similar structures subserve at least one fundamental physiologic function: rapid and efficient transport over complex, spatially distributed networks. It seems there is a gradual loss of complexity in these structures due to age or disease. The difference between a healthy and a sick heart may become evident with fractal analysis. The study described in the article "Fractal diagnosis of severe cardiac dysfunction. Fractal dynamic of the left coronary branching" [12] shows that a healthy heart exhibits a non-zero fractal dimension with a wide range of variability, whereas a heart presenting an arterial obstruction displayed a lower and less variable fractal dimension.

7.2 Age group classification

Human face analysis provides much information and is the topic of many investigations. In a study carried out in King Saud University [14], a novel method for human age group classification based on the Correlation Fractal Dimension of facial edges is described. With age there are changes in internal bone structure, a loss of elasticity of the skin and a loss of sub cutaneous fat. These factors constitute age-invariant signatures of faces. The above changes manifest in the form of facial wrinkles and facial edges. Previously, no study

has attempted to classify the facial image of humans into four categories based on the Fractal Dimension value. In the study the images were cut and converted to grayscale (see Figure 7.2) and the facial edge was extracted using the canny edge operator, and finally, the correlation between the Fractal Dimension of various parameters was calculated, thus classifying the age group of each image with a very high degree of accuracy (see Figure).

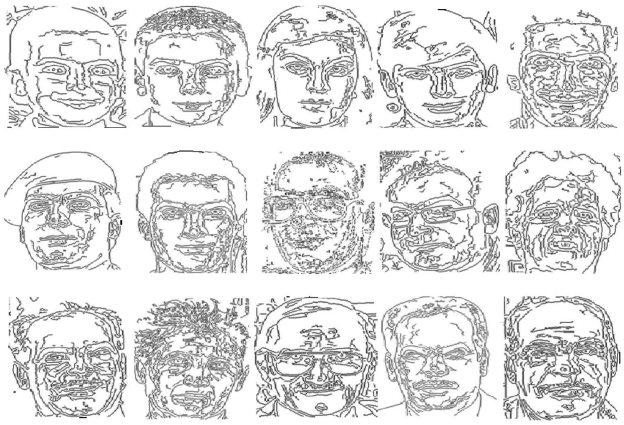

Figure 7.1: Grayscale faces.

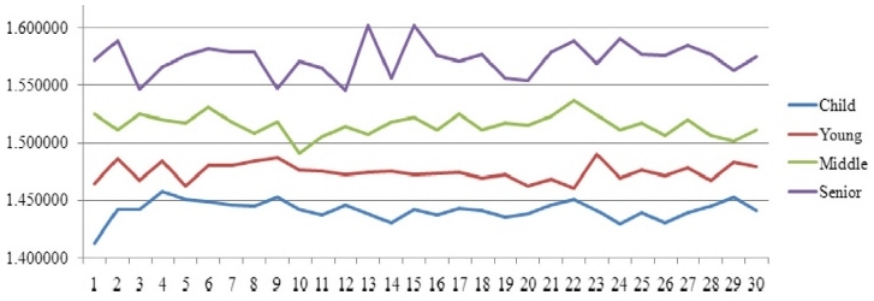

Figure 7.2: Classification graph of age group classification based on the proposed method.

7.3 Meteorological quantities

This next project, carried out in the Czech Republic [7], attempted to ascertain the relation between the fractal dimension of micro-meteorologic characteristics and thermodynamics of the atmosphere, and the development of biodiversity and the violation of the Small Water Cycle (SWC). The research data from 15 measuring centers in the Trebon region was collected into the database, placed in a time series, and its fractal dimension was calculated using the box counting method. Each of the centers measured 13 meteorological variables like a temperature in 2 meters and 30 centimeters above surface, humidity (in the same altitude), solar radiation and the radiation reflected from

earth surface, rainfall, wind speed and direction and temperature and humidity of the earth in different depth. The data from these measuring centers was saved into the database with a 5 minute period. The measuring points were categorized into group according to their surface (meadow, tideland, pond, field, concrete surface etc.).

The experimental results showed that the fractal dimension of micro-meteorological quantities has a relation to the environmental factors. E.g., fractal dimension of the earth temperature under the concrete surface (where the violation of the SWC is expected) was found to be significantly lower than a fractal dimension from pasture and above the earth surface vice versa.

7.4 Stock Market

The article "Computing the fractal dimension of stock market indices"[9]. shows that the stock market can be analyzed as a fractal and assigned a fractal dimension. The fractal structure of the stock market comes in contrast with the Efficient Market Hypothesis, which assumes that markets follow a random walk, making the impact of any new information essentially unpredictable. Rescaled range (R/S) analysis shows that the stock market, like many other systems, is not completely random, but has a long term memory that links patterns in its behavior over time, giving it a fractal structure. To analyze the stock market's fractal structure, we have to view it as a time series, or a series of points spaced out evenly in time, each having a value that corresponds to the behavior of the stock market at that point in time.

The article concludes that chaos theory can be applied to assign order and detect patterns even in seemingly random systems, such as the stock market and that analysis of the fractal dimension of the stock market as a whole may eventually lead the way to prediction of the market's behavior.

7.5 Shopping Paths

The usage of fractal dimensions extends over many and diverse fields, reaching even the most daily activities such as shopping. A study published in the journal *Procedia Computer Science[8]* intends to demonstrate the influence of shopping paths in a supermarket on purchase behavior. It uses fractal dimension to quantify the complexity of customer shopping paths, then relating it to mean volume of purchase and stay time in store.

1000 customers in a supermarket in Japan were analyzed and divided into two groups, according to the fractal dimension of the path (high and low). Focusing on the sales amount analysis results, it seems that more products were purchased when there was strong complexity and randomness of the customer in-store movements (high fractal dimension). Specifically, the stay time in store resulted in a difference of more than double; people in the high fractal dimension customer group tended to have a longer shopping time.

Islands in the sea of complexity

To appreciate the nature of fractals, recall Galileo's splendid manifesto that "Philosophy is written in the language of mathematics and its characters are triangles, circles and other geometric figures, without which one wanders about in a dark labyrinth." Observe that circles, ellipses, and parabolas are very smooth shapes and that a triangle has a small number of points of irregularity. Galileo was absolutely right to assert that in science those shapes are necessary. But they have turned out not to be sufficient, "merely" because most of the world is of infinitely great roughness and complexity. However, the infinite sea of complexity includes two islands: one of Euclidean simplicity, and also a second of relative simplicity in which roughness is present, but is the same at all scales.

From the interview *A theory of roughness* with B. Mandelbrot [12.19.04]

References

[1] Barnsley, M. F. *Fractals everywhere*. Academic press, 2014.

[2] Besicovitch, A., and Ursell, H. Sets of fractional dimensions (v): On dimensional numbers of some continuous curves. *Journal of the London Mathematical Society* (1937).

[3] Billingsley, P. *Probability and measure*. John Wiley & Sons, 2008.

[4] Falconer, K. *Fractal geometry: mathematical foundations and applications*. John Wiley & Sons, 2004.

[5] Frame, M., Mandelbrot, B., and Neger, N. `http://users.math.yale.edu/public_html/People/frame/Fractals`, 2017-06-08.

[6] Hunter, J. K., and Nachtergaele, B. *Applied analysis*. World Scientific Publishing Co Inc, 2001.

[7] Jura, J., and Bila, J. Computation of the fractal dimension of meteorological quantities. In *Proceedings of 16th International Conference on Soft ComputingâMendel* (2010), pp. 140–145.

[8] Kaneko, Y., and Yada, K. Fractal dimension of shopping path: Influence on purchase behavior in a supermarket. *Procedia Computer Science 96* (2016), 1764–1771.

[9] Kompella, M. Computing the fractal dimension of stock market indices. *COSMOS* (2014).

[10] Mandelbrot, B. B. How long is the coast of britain. *Science* (1967).

[11] Mandelbrot, B. B., and Pignoni, R. *The fractal geometry of nature*, vol. 173. WH freeman, 1983.

[12] Rodríguez, J. O., Prieto, S. E., Correa, S. C., Bernal, P. A., Tapia, D., Álvarez, L. F., Mora, J. T., Vitery, S. M., and Salamanca, D. G. Diagnóstico fractal de disfunción cardiaca severa. dinámica fractal de la ramificación coronaria izquierda. *Revista Colombiana de Cardiología 19*, 5 (2012), 225–232.

[13] Wolfram MathWorld. `http://www.mathworld.wolfram.com`, 2017-06-01.

[14] Yarlagadda, A., Murthy, J., and Prasad, M. K. A novel method for human age group classification based on correlation fractal dimension of facial edges. *Journal of King Saud University-Computer and Information Sciences 27*, 4 (2015), 468–476.